JOC The Journal of Organic Chemistry

Article

pubs.acs.org/joc

Computational and Experimental Studies of Regioselective S_NAr Halide Exchange (Halex) Reactions of Pentachloropyridine

Robert D. J. Froese,*[,†] Gregory T. Whiteker,*[,‡] Thomas H. Peterson,[†] Daniel J. Arriola,[†] James M. Renga,[‡] and Justin W. Shearer[‡]

[†]The Dow Chemical Company, 1776 Building, Midland, Michigan 48674, United States

[‡]Dow AgroSciences, 9330 Zionsville Road, Indianapolis, Indiana 46268, United States

Supporting Information

ABSTRACT: The Halex reaction of pentachloropyridine with fluoride ion was studied experimentally and computationally with a modified ab initio G3MP2B3 method. The G3 procedure was altered, as the anionic transition state optimizations failed due to the lack of diffuse functions in the small 6-31G* basis set. Experimental Halex regioselectivities were consistent with kinetic control at the 4-position. The reverse Halex reaction of fluoropyridines with chloride sources was demonstrated using precipitation of LiF in DMSO as a driving force. Reverse Halex regioselectivity at the 4-position was predicted by computations and was consistent with kinetic control. Scrambling of halide ions between chlorofluoropyridines was catalyzed by *n*-Bu_4PCl, and the products of these reactions were shown to result from a combination of kinetic and thermodynamic control. Comparison of the C−F and C−Cl homolytic bond dissociation energies suggests that an important thermodynamic factor which controls regioselectivity in this system is the weak C2−Cl bond. The differences between $\Delta H°$ values of chlorofluoropyridines can be explained by a combination of three factors: (1) the number of fluorine atoms in the molecule, (2) the number of fluorine atoms at the C2 and C6 positions, and (3) the number of pairs of fluorine atoms which are ortho to one another.

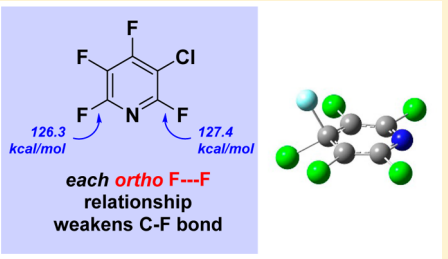

INTRODUCTION

Incorporation of fluorine is a common strategy used by pharmaceutical and agrochemical chemists to improve the efficacy of bioactive molecules.[1,2] Properties such as lipophilicity, solubility, rate of absorption, and stability toward metabolism can be tailored by substitution with fluorine.[3,4] Many modern crop protection chemicals have fluorinated structures, and herbicides in particular often contain fluorine substituents.[5] The synthesis of fluorinated organic compounds can be performed by a variety of routes.[6] The extreme reactivity of elemental fluorine makes direct fluorination useful for only a small number of substrates. The two main routes that are utilized industrially for the synthesis of the majority of fluoroarenes and fluoroheteroarenes are the Schiemann reaction and the Halex reaction. The Schiemann reaction, which involves diazotization of aromatic amines in anhydrous HF and subsequent decomposition of the resultant aryldiazonium fluorides (or tetrafluoroborates), is widely used. The Halex or halogen exchange reaction is, however, the most preferred process to form aromatic C−F bonds.[7] In this process, a chloroarene is converted to a fluoroarene via nucleophilic aromatic substitution (S_NAr) with a fluoride salt. Typically, Halex reactions are performed at high temperatures (≥150 °C) in polar, nonprotic solvents such as DMSO and DMF.[8] Use of so-called "naked fluoride" sources, e.g., anhydrous tetrabutylammonium fluoride (N(*n*-Bu)$_4$F) and tetramethylammonium fluoride (NMe_4F),[9] give high reactivities in Halex reactions at much lower temperatures, although the expense of these reagents limits their widespread commercial use.

Halex reactions function by a nucleophilic aromatic substitution mechanism, or addition−elimination S_NAr mechanism,[10,11] which typically requires the presence of an electron-withdrawing activating group on the aromatic ring to allow reactions to be performed at a synthetically useful temperature. In the absence of an activating group, Halex reactions occur only under harsh reaction conditions.[12] In systems containing an activating (i.e., electron-withdrawing) group, the halide will add at positions ortho and para to the activating group, resulting in an intermediate wherein a developing negative charge can be stabilized by the activating group via resonance. The lack of resonance stabilization in intermediates resulting from addition at the meta position results in slower reaction rates for the formation of meta products and accounts for the general lack of reaction at the meta position except under forcing conditions. Many Halex reactions that are practiced commercially involve an exhaustive substitution of all chloride substituents. However, regioselective, partial Halex reactions of polychlorinated aromatics can be performed when an activating group strongly directs the position of attack by fluoride.

Examples of agrochemicals which are produced using Halex reactions are shown in Figure 1. Clodinafop can be prepared from 5-chloro-2,3-difluoropyridine via a regioselective Halex

Received: July 10, 2016

DOI: 10.1021/acs.joc.6b01656
J. Org. Chem. XXXX, XXX, XXX−XXX

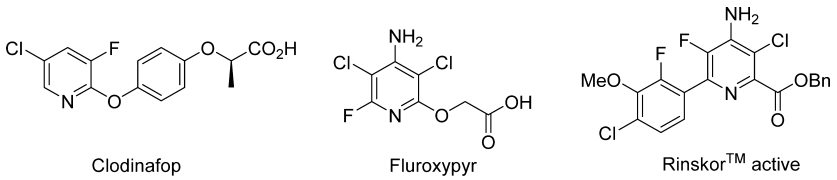

Figure 1. Examples of herbicides which contain fluoropyridine moieties.

reaction of either 2,3,5-trichloropyridine or 2,5-dichloro-3-fluoropyridine.[5] Similarly, a regioselective Halex reaction of pentachloropyridine is utilized in the manufacture of 3,5-dichloro-2,4,6-trifluoropyridine, which is an intermediate in the synthesis of the commercial broadleaf herbicide Fluroxypyr.[5]

As part of process chemistry research on the new rice herbicide, Rinskor active,[13,14] we were interested in understanding the factors which could enable regioselective introduction of the 5-fluoride substituent on the pyridine ring using Halex chemistry. As our entry into this area, we performed a detailed ab initio computational and experimental study to understand the kinetics and thermodynamics of the commercially important Halex reaction of pentachloropyridine. Kinetic barriers for halogen exchange of each individual C−Cl bond in every potential intermediate were calculated for the exhaustive substitution to give ultimately pentafluoropyridine. These calculated barriers were compared to the experimental data derived under kinetic control. Reaction enthalpies were also computed for comparison to experimental results. These results indicated that the regioselectivity of Halex reactions of pentachloropyridine is kinetically controlled. At higher temperatures, an equilibration process exists which allows some chlorofluoropyridine isomers to interconvert. The factors which control the regioselectivity of this interconversion are discussed, as well as a new reverse-Halex reaction which is driven by insolubility of LiF in DMSO. A complete computational investigation led to the development of the key factors which control thermodynamic regioselectivity in this system. In addition, during the course of our computational studies, a limitation of the high-level theoretical ab initio method G3MP2B3 was uncovered and addressed.

RESULTS AND DISCUSSION

Experimental Study of the Kinetics of the Halex Reaction of Pentachloropyridine. The Halex reaction of pentachloropyridine ($\mathbf{F_0}$) to form 3,5-dichloro-2,4,6-trifluoropyridine ($\mathbf{2,4,6\text{-}F_3}$, Figure 2) is employed in the manufacture of the herbicide Fluroxypyr. The use of KF in polar solvents near 200 °C leads to regioselective formation of $\mathbf{2,4,6\text{-}F_3}$.[15,16]

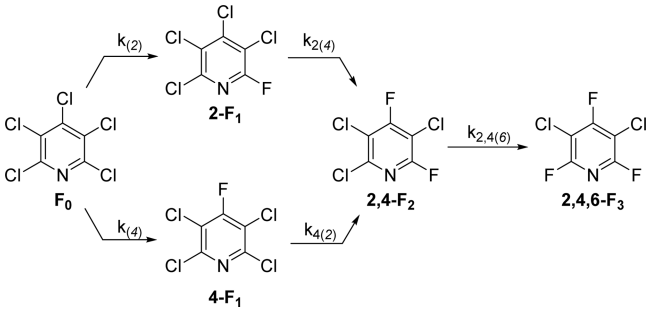

Figure 2. Experimentally observed products in the Halex reaction of $\mathbf{F_0}$ with TASF.

Undesired, subsequent Halex reactions of $\mathbf{2,4,6\text{-}F_3}$ at the 3- and 5-positions to produce 5-chloro-2,3,4,6-tetrafluoropyridine ($\mathbf{2,3,4,6\text{-}F_4}$) and pentafluoropyridine ($\mathbf{F_5}$) are much slower under these conditions, due to the known ortho/para activating influence of the heterocyclic nitrogen atom. Although the sequence of Halex reactions to form $\mathbf{2,4,6\text{-}F_3}$ must proceed through monofluoro and difluoro intermediates, little information is available on which intermediate isomers are involved. One report in the patent literature[17] described the synthesis of 3,4,5,6-tetrachloro-2-fluoropyridine ($\mathbf{2\text{-}F_1}$) from the Halex reaction of $\mathbf{F_0}$ with KF in sulfolane at 230 °C, whereas 2,3,5,6-tetrachloro-4-fluoropyridine ($\mathbf{4\text{-}F_1}$) was the product obtained using CsF and 18-crown-6 in acetonitrile at 80 °C.[18] On the basis of these results, it is likely that $\mathbf{2\text{-}F_1}$ is the thermodynamically preferred monofluorinated isomer, whereas the $\mathbf{4\text{-}F_1}$ isomer is the kinetic product formed at lower temperatures.

To improve our understanding of the regioselectivities of these stepwise reactions, we sought to determine the nature of the intermediate chlorofluoropyridines by performing the Halex reaction under conditions where product distributions were most likely under kinetic control. The Halex reaction of $\mathbf{F_0}$ was conducted in THF at 26 °C using the rigorously anhydrous "naked fluoride" source $[(Me_2N)_3S](Me_3SiF_2)$ (TASF).[19] This soluble fluoride source was chosen to avoid potential complications caused by partial solubility. Under these conditions, Halex reactions of $\mathbf{F_0}$ proceeded rapidly upon mixing and gave a mixture of intermediate chlorofluoropyridines whose relative concentrations were determined by ^{19}F NMR spectroscopy (Table 1). Efforts to obtain kinetic

Table 1. Product Distributions for the Reaction of TASF with $\mathbf{F_0}$ in THF

	product distribution (%)			
amt of TASF (equiv)	2-F	4-F	2,4-F_2	2,4,6-F_3
0.33	18.2	69.7	12.2	0
0.50	17.9	67.9	14.3	0
1.0	11.5	45.1	38.2	5.3
2.0	1.7	16.2	51	31
3.0	0.3	1	13.7	85.1

information were hampered by the speed of the reactions. Further attempts to slow these reactions by using less polar solvents (toluene-d_8, CD_2Cl_2) were precluded by either the insolubility of pentachloropyridine or by the reactivity of TASF with these solvents. When 1.0 equiv of TASF was used, a mixture containing 11.5% $\mathbf{2\text{-}F_1}$, 45.1% $\mathbf{4\text{-}F_1}$, 38.2% $\mathbf{2,4\text{-}F_2}$, and 5.3% $\mathbf{2,4,6\text{-}F_3}$ was observed.[20] The formation of a mixture of mono-, di-, and trifluoro products using only 1 equiv of TASF indicated that the rates of the first three reactions were comparable. Experiments using 0.33 and 0.50 equiv of TASF gave mixtures containing $\mathbf{2\text{-}F_1}$ and $\mathbf{4\text{-}F_1}$ and a small amount of $\mathbf{2,4\text{-}F_2}$. From the relative amounts of $\mathbf{2\text{-}F_1}$ and $\mathbf{4\text{-}F_1}$ formed, it is

DOI: 10.1021/acs.joc.6b01656
J. Org. Chem. XXXX, XXX, XXX−XXX

apparent that the Halex reaction at the 4-position (para to the pyridine nitrogen) was faster than substitution at the 2-position (ortho to the pyridine nitrogen). Likewise, the absence of **2,6-F_2** indicated that the rate of substitution at the 6-position in **2-F_1** ($k_{2(6)}$) was relatively slow. Similar regioselectivities have been reported for the nucleophilic aromatic substitution of pentachloropyridine with ammonia and alkoxides.[21] No products from substitution at the 3-position (meta to the pyridine nitrogen) were observed under these conditions due to the higher kinetic barrier for substitution. When 3.0 equiv of TASF was used, ^{19}F NMR showed the presence of 85.1% **2,4,6-F_3** along with 13.7% **2,4-F_2** and ≤1% of **2-F_1** and **4-F_1**. No tetrafluorochloro isomers or pentafluoropyridine was observed. Since both **2-F_1** and **4-F_1** reacted quickly, the best estimate of kinetic reactivity at these positions was with the lowest amount of added fluoride, 0.33 equiv of TASF. Under these conditions, the **4-F_1**:**2-F_1** ratio is 3.8, which indicated a kinetic preference at the 4-position by 7.6.

Computational Study of the Kinetics and Thermodynamics of the Halex Reaction of Pentachloropyridine. The exhaustive Halex process leading from F_0 to F_5 was studied computationally using density functional theory (DFT, B3LYP/6-311+G**) and high level ab initio methods (G3MP2B3) with specifics provided in the Computational Details and Supporting Information. Figure 3 shows the structures

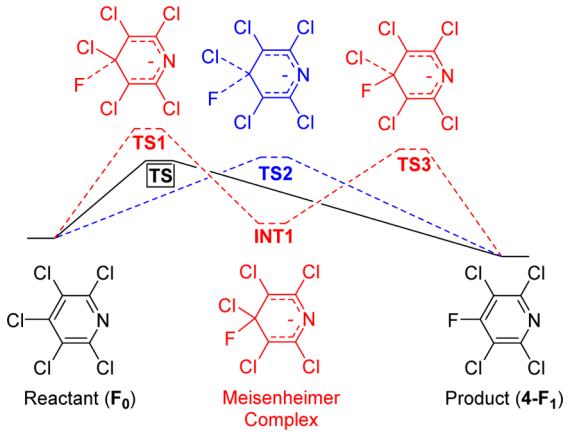

Figure 3. Concerted (dashed blue line), stepwise (dashed red line), and actual computed (solid black line) mechanisms for fluoride exchange at the 4-position of pentachloropyridine, F_0.

evaluated on the potential energy surface for fluoride attack at the 4-position of F_0. The red dashed line depicts **4-F_1** product formation via a hypothetical Meisenheimer complex (**INT1**) formed from an early transition state (**TS1**) with little distortion of the C−Cl bond. **INT1** would lead to product via **TS3**, characterized by a lengthened C−Cl bond. The blue dashed line represents a concerted process for halide exchange that occurs via a more symmetrical transition state (**TS2**) characterized by a forming C−F bond and a lengthened C−Cl bond. Of the four transition state and intermediate structures depicted, only a single transition state structure (**TS**) could be located computationally. This structure possessed a lengthened C−F bond with little distortion of the C−Cl bond and resembled **TS1**. However, this structure collapsed directly to **4-F_1** without intervention of a detectable Meisenheimer complex or second transition state, likely indicating a concerted reaction pathway for substitution (solid black line in Figure 3). Important geometrical features of this early transition state are shown in the Supporting Information. Our inability to locate an intermediate in the first Halex reaction of F_0 is in agreement with other computational reports which showed that the presence of Meisenheimer complexes is dependent on the nucleophile and leaving group.[22−25] For S_NAr reactions that involve a fluoride leaving group, these previous computational studies have shown the presence of the Meisenheimer complex **INT1**, whereas S_NAr reactions with a chloride leaving group proceed through **TS2**.

While thorough details of the calculations are provided in the Computational Details and Supporting Information, one particularly interesting limitation of the theoretical method deserves mention. Transition state structures were initially optimized at the B3LYP/6-311+G** level of theory with the PCM solvation model (DMSO). Attempts to utilize the high-level G3MP2B3 method for accurate energy calculations (PCM included) failed to optimize the geometries of the anionic transition states due to this method's use of a modest B3LYP/6-31G* basis set.[26] It is curious that, while the most computationally intensive part of the G3MP2B3 method is QCISD(T)/6-31G*, the geometry optimizations and frequencies use an extremely small basis set, 6-31G*. We propose it is more appropriate to use a larger basis set for optimizations and frequency calculations.[27] Due to the failure of the geometry optimizations, the automated G3 procedures within Gaussian could not be used, and the separate calculations associated with the G3MP2B3 enthalpies were computed independently and summed on the basis of the B3LYP/6-311+G** geometries. The G3MP2B3 calculations can be reduced to a high-level/modest basis set term, QCISD(T)/6-31G*, with a basis set correction from perturbation theory, ΔMP2 = MP2/6-311++G(2df,2p) − MP2/6-31G*. For highest accuracy, the basis set correction term (ΔMP2) should be small, but because the 6-31G* basis set was shown to be inadequate for our transition state optimizations, these correction terms (ΔMP2) were extremely large. Since it is known that diffuse functions are beneficial for anions,[27] we created a new method referred to as G3MP2B3*, where the high-level method used was QCISD(T)/6-31+G* with the basis set correction: ΔMP2* = MP2/6-311++G(2df,2pd) − MP2/6-31+G*. This improvement in the high-level basis set dramatically reduced the correction error (ΔMP2*) and presumably made these calculations more accurate. The resulting G3MP2B3* enthalpies were used to investigate the Halex reactions from F_0 to F_5 (Table 2). The structures and computed energies obtained using different computational methods are tabulated in the Supporting Information.

Ab initio calculations were performed for the exhaustive Halex reaction at every position and in all possible reaction sequences. Enthalpies of activation can be calculated mathematically from the data in Table 2. As an illustration, the activation enthalpy for reaction of fluoride at the 2-position of **4-F_1** (12.4 kcal/mol) is obtained by subtracting the computed energy of the **4-F(2)** transition state (−3.7 kcal/mol) from the computed enthalpy of **4-F_1** (−16.1 kcal/mol). Similarly, the relative energy of any reaction, isomerization, or barrier can be computed by comparing the energies of the appropriate species from Table 2. As described in the following sections, the calculated energies of these intermediates and transition states accurately explained the observed reactivity patterns. Experimental results showed that the 3- and 5-chloride substituents were much less reactive than those at the 2-, 4-, and 6-positions. For the first three fluoride exchanges, no

DOI: 10.1021/acs.joc.6b01656
J. Org. Chem. XXXX, XXX, XXX−XXX

Table 2. Energies (Relative to F_0) for All Intermediates and Transition States (TSs) for the Halex Reaction of Pentachloropyridine[a]

Pentachloropyridine Minimum				
F_0: 0.0				
Pentachloropyridine TSs				
F_0(*2*): 12.5	F_0(*3*): 17.9	F_0(*4*): 11.5		
Monofluorinated Minima				
2-F$_1$: -19.5	**3-F$_1$**: -15.1	**4-F$_1$**: -16.1		
Monofluorinated TSs				
2-F$_1$(*3*): -0.2	**2-F$_1$**(*4*): -8.1	**2-F$_1$**(*5*): 0.9	**2-F$_1$**(*6*): -7.2	**3-F$_1$**(*2*): -2.5
3-F$_1$(*4*): -3.0	**3-F$_1$**(*5*): 2.4	**3-F$_1$**(*6*): -0.9	**4-F$_1$**(*2*): -3.7	**4-F$_1$**(*3*): 3.3
Difluorinated Minima				
2,3-F$_2$: -33.1	**2,4-F$_2$**: -35.4	**2,5-F$_2$**: -34.4	**2,6-F$_2$**: -38.9	**3,4-F$_2$**: -29.6
3,5-F$_2$: -30.0				
Difluorinated TSs				
2,3-F$_2$(*4*): -21.2	**2,3-F$_2$**(*5*): -13.4	**2,3-F$_2$**(*6*): -19.3	**2,4-F$_2$**(*3*): -14.3	**2,4-F$_2$**(*5*): -13.5
2,4-F$_2$(*6*): -23.2	**2,5-F$_2$**(*3*): -15.5	**2,5-F$_2$**(*4*): -22.7	**2,5-F$_2$**(*6*): -21.4	**2,6-F$_2$**(*3*): -16.8
2,6-F$_2$(*4*): -27.5	**3,4-F$_2$**(*2*): -16.4	**3,4-F$_2$**(*5*): -10.7	**3,4-F$_2$**(*6*): -15.6	**3,5-F$_2$**(*2*): -14.9
3,5-F$_2$(*4*): -17.0				
Trifluorinated Minima				
2,3,4-F$_3$: -47.9	**2,3,5-F$_3$**: -48.1	**2,3,6-F$_3$**: -52.6	**2,4,5-F$_3$**: -48.8	**2,4,6-F$_3$**: -54.7
3,4,5-F$_3$: -43.2				
Trifluorinated TSs				
2,3,4-F$_3$(*5*): -26.5	**2,3,4-F$_3$**(*6*): -34.1	**2,3,5-F$_3$**(*4*): -35.3	**2,3,5-F$_3$**(*6*): -33.2	**2,3,6-F$_3$**(*4*): -40.7
2,3,6-F$_3$(*5*): -31.0	**2,4,5-F$_3$**(*3*): -28.1	**2,4,5-F$_3$**(*6*): -35.8	**2,4,6-F$_3$**(*3*):-30.9	**3,4,5-F$_3$**(*2*): -28.3
Tetrafluorinated Minima				
2,3,4,5-F$_4$: -61.4	**2,3,4,6-F$_4$**: -67.1	**2,3,5,6-F$_4$**: -66.2		
Tetrafluorinated TSs				
2,3,4,5-F$_4$(*6*): -46.5	**2,3,4,6-F$_4$**(*5*): -43.7	**2,3,5,6-F$_4$**(*4*): -53.5		
Pentafluoropyridine Minimum				
F_5: -79.6				

[a]Enthalpies are given in kcal/mol at the high-level, modified G3MP2B3* method. The position of attack in the transition states is denoted in parentheses. The kinetic path predicted for the forward Halex reaction of F_0 for each sequential, lowest energy transition state is highlighted in red. The kinetic pathway predicted for the reverse Halex reaction of F_5 is highlighted in green.

meta-fluorinated transition states were comparable in energy to their ortho- or para-fluorinated isomers. The enthalpies of activation for each of the first three Halex substitutions at the 2-, 4-, and 6- positions were all within 1 kcal/mol. The similarity of these barriers was consistent with the observed mixture of **2-F$_1$**, **4-F$_1$**, **2,4-F$_2$**, and **2,4,6-F$_3$** in the Halex reaction of F_0 with 1 equiv of TASF. For the first Halex reaction of F_0, we calculated enthalpies of activation of 12.5, 17.9, and 11.5 kcal/mol for reaction at the 2-, 3-, and 4-positions, respectively. The Halex reaction at the 3-position of F_0 was calculated to have a barrier 6.4 kcal/mol higher than the barrier for substitution at the 4-position and was consistent with the complete absence of **3-F$_1$** experimentally. Subsequent halogen exchange reactions at the 3- and 5-positions of intermediate chlorofluoropyridines had similarly high barriers. The barrier to the Halex reaction at the 2-position of F_0 ($\Delta H^{\ddagger}$ = 12.5 kcal/mol) was only 1.0 kcal/mol higher than the barrier for reaction at the 4-position. This computed $\Delta\Delta H^{\ddagger}$ value was consistent with results from experiment, which showed that the relative rate constant for formation of **4-F$_1$** was 7.6 times faster than the rate constant to produce **2-F$_1$**. At 25 °C, a factor of 7.6 corresponds to a 1.2 kcal/mol energy difference between transition states, in excellent agreement with the computed values. Although **4-F$_1$** was kinetically favored over **2-F$_1$**, the 2-fluoro isomer has an enthalpy of reaction (ΔH°) which was 3.4 kcal/mol lower than that of **4-F$_1$**. The 3-fluoro isomer **3-F$_1$** was the least stable of the monofluorinated isomers, with a ΔH° value which was 4.4 kcal/mol higher than that of **2-F$_1$**. Our calculations showed that there is a large thermodynamic preference for structures which contain fluorine substituents ortho to the pyridine nitrogen. Therefore, the previously reported synthesis of **2-F$_1$** from the Halex reaction of F_0 and KF at 230 °C[17] was most likely under thermodynamic control via a mechanism which allowed isomerization to occur.

For the second set of halogen exchange reactions, only the pathways which involved reaction at the 2- and 4-positions are discussed, although all possible substitutions were studied computationally. Any further reaction of **3-F$_1$** would not contribute to the product distribution due to the high kinetic barrier to its formation. The kinetically favored, monofluoro intermediate **4-F$_1$** was predicted to react with fluoride at the 2-position to form **2,4-F$_2$** with $\Delta H^{\ddagger}$ = 12.4 kcal/mol. The minor monofluoro intermediate **2-F$_1$** would react at the 4- or 6-position with a barrier of 11.4 or 12.3 kcal/mol, respectively. The Halex reaction of **2-F$_1$** would therefore, like **4-F$_1$**, also preferentially lead to **2,4-F$_2$**. A further Halex reaction of **2,4-F$_2$** selectively led to **2,4,6-F$_3$** with a calculated barrier of 12.2 kcal/mol. In addition to being kinetically preferred, **2,4,6-F$_3$** is also the thermodynamically favored trifluorinated isomer. The further Halex reaction of **2,4,6-F$_3$** to give **2,3,4,6-F$_4$** was calculated to have a barrier of 23.8 kcal/mol, which is >10 kcal/mol higher than those of the previous three fluoride substitutions. This barrier was consistent with the absence of any tetrafluorinated isomer in our experiments using 3.0 equiv of TASF. The final Halex reaction to form pentafluoropyridine had a similarly high barrier of 23.4 kcal/mol. Experimental results in the literature[15] indicate that further Halex reactions of **2,4,6-F$_3$** only occur under forcing conditions, consistent with the larger barriers computed for these reaction steps. Indeed, it is this relative lack of reactivity of the 3- and 5-chloride substituents that makes this reaction useful for the commercial synthesis of Fluroxypyr, which proceeds via **2,4,6-F$_3$**.

Reverse Halex Reactions of Fluoropyridines. During Halex reactions aimed at the synthesis of Rinskor active, we observed experimental indications of potential reversion of

DOI: 10.1021/acs.joc.6b01656
J. Org. Chem. XXXX, XXX, XXX−XXX

fluoropyridines to chloropyridines at extended reaction times.[28] Although these reverse Halex reactions were calculated to be endothermic by >15 kcal/mol, we speculated that precipitation of an insoluble fluoride salt might be used experimentally to drive the reaction backward to more chlorinated products. This type of reverse Halex reaction would be analogous to the classic Finkelstein reaction, which uses the differential solubilities between NaI and NaCl in acetone as the driving force to prepare iodoalkanes. Such reverse Halex reactions could potentially be used to prepare regioisomers that were not accessible from the forward reaction and could also possibly be utilized to recycle overfluorinated byproducts of Halex reactions. On the basis of the dramatic differences in water solubilities of alkali-metal chloride and fluoride salts (Table 3),[29] we hypothesized that precipitation of LiF, in particular,

Table 3. Solubilities of Halide Salts in Water and DMSO at 20 °C

	solubility (mg/mL)	
salt	H_2O[a]	DMSO
LiF	1.34	<0.0001
LiCl	447	94 ± 12
NaF	39.7	<0.0001
NaCl	263	4.4 ± 0.6

[a]Reference 31.

could be used as a driving force for reverse Halex reactions. Since Halex reactions are not typically compatible with the presence of water, we determined the solubility of these same halide salts in anhydrous DMSO. Ion chromatography confirmed that LiF and NaF were indeed practically insoluble in DMSO (Table 3). In addition, LiCl was found to have significantly higher solubility than NaCl in DMSO. The rates of the reverse Halex reactions of **2,4,6-F_3** with different chloride salts in DMSO are compared in Figure 4. Negligible reaction was observed by gas chromatography using 2.5 equiv of NaCl in DMSO at 100 °C. By comparison, almost complete conversion of **2,4,6-F_3** to 3,4,5-trichloro-2,6-difluoropyridine (**2,6-F_2**) occurred after 9 h at 100 °C using 2.5 equiv of LiCl in DMSO. No other difluoro isomers were observed. This difference in reactivity between LiCl and NaCl was consistent with the significantly higher solubility of LiCl in DMSO. The use of bis(triphenylphosphine)iminium chloride (PPNCl) led to only partial conversion to **2,6-F_2**. No precipitation of bis(triphenylphosphine)iminium fluoride was observed from DMSO, and this reactivity may instead be driven by the covalent nature of PPNF.[30] When the reaction of **2,4,6-F_3** with 1 equiv of LiCl was conducted on a preparative scale, **2,6-F_2** was isolated in 53% yield. By taking advantage of the lower solubility of LiF in DMSO, the reverse Halex reaction could, indeed, be performed.

The regiochemistries of the difluoro products prepared by Halex and reverse Halex reactions were observed to be different but were consistent with the kinetic preference for substitution at the 4-position. In the case of the forward Halex reaction of **F_0** with TASF, **2,4-F_2** was the sole observed difluoro isomer. This selectivity was due to the lower $\Delta H^{\ddagger}$ value for the first fluoride substitution at the 4-position over the 2- and 3-positions (Figure 5), followed by reaction with a second equivalent of

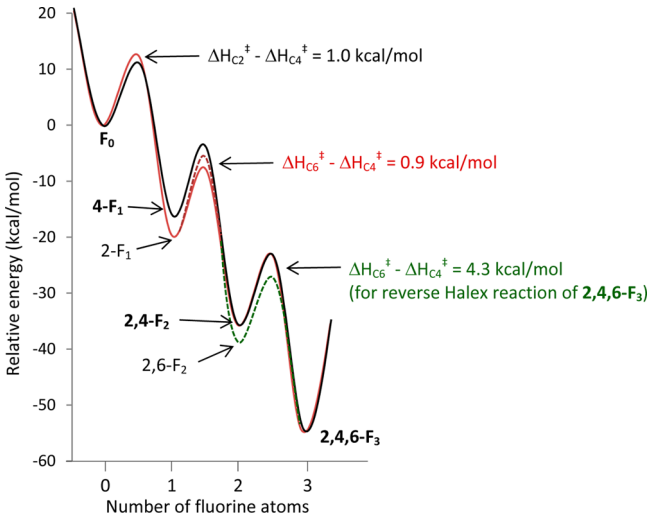

Figure 5. Calculated reaction coordinate for the Halex reactions of fluoride ion with **F_0** to give **2,4,6-F_3**. The solid black line depicts the kinetically dominant pathway via **4-F_1** and **2,4-F_2**. The minor monofluoro isomer **2-F_1** reacts preferentially ($\Delta\Delta H^{\ddagger}$ = 0.9 kcal/mol) with fluoride at the 4-position over the 6-position to give **2,4-F_2**. The reverse Halex pathway for reaction of chloride with **2,4,6-F_3** to give **2,6-F_2** is shown as a green dashed line.

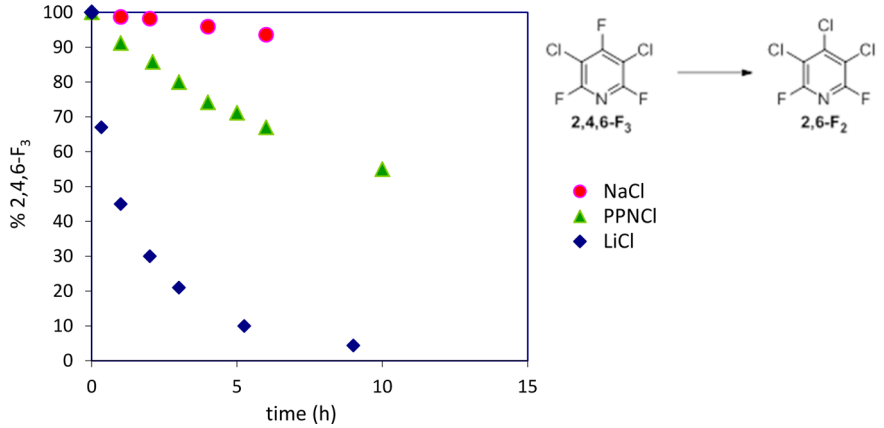

Figure 4. Effect of counterion on the reverse Halex reaction of chloride salts (Li, blue ◆; Na, red ●; PPN, green ▲) with **2,4,6-F_3** to give **2,6-F_2** (100 °C, 1 M in DMSO, 2.5 equiv of chloride salt).

DOI: 10.1021/acs.joc.6b01656
J. Org. Chem. XXXX, XXX, XXX−XXX

fluoride to give **2,4-F$_2$**. If any **2-F$_1$** was formed in the reaction with **F$_0$**, it would be expected to react with additional fluoride at the 4-position to also give **2,4-F$_2$**. For the reverse Halex reaction of **2,4,6-F$_3$** with chloride, the 4-position was calculated to be kinetically dominant over the 2-position ($\Delta\Delta H^{\ddagger}$ = 4.3 kcal/mol) to exclusively produce the **2,6-F$_2$** isomer. The forward Halex reactions favored 4-substitution over 2-substitution by fluoride, typically by only ~1 kcal/mol. However, the reverse Halex reactions favored 4-substitution over 2-substitution by chloride, often by more than 4 kcal/mol, and were very selective. In addition to being the kinetic product, **2,6-F$_2$** was also the thermodynamically favored isomer in the reverse Halex reaction of **2,4,6-F$_3$** by 3.5 kcal/mol.

To confirm that the regioselectivity of the reverse Halex reaction was indeed kinetically controlled, the reaction of **F$_5$** with LiCl in DMSO was studied, since the thermodynamic and kinetic monofluoro isomers were calculated to be different. For the reverse Halex reaction of **F$_5$**, the kinetically preferred product (by 7.0 kcal/mol) was predicted to be **2,3,5,6-F$_4$**, formed by substitution of chloride at the 4-position (Figure 6).

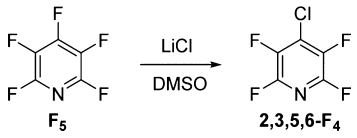

F$_5$ **2,3,5,6-F$_4$**

Figure 6. Reverse Halex reaction of **F$_5$** with LiCl in DMSO (80 °C, 1 M).

Thermodynamic control would be expected to form a mixture of **2,3,4,6-F$_4$** and **2,3,5,6-F$_4$** ($\Delta\Delta H°$ = 0.9 kcal/mol). Experimentally, **2,3,5,6-F$_4$** was found to be the sole product of reaction of **F$_5$** with LiCl in DMSO at 80 °C and was consistent with the reverse Halex regioselectivity being kinetically determined. The reaction of **F$_5$** with $CaCl_2$ and DCH-18-crown-6 in refluxing sulfolane was previously reported to give **2,3,5,6-F$_4$** and likely proceeds via a S_NAr mechanism.[31] Our results suggest that the reverse Halex reaction of fluorinated pyridines with LiCl in DMSO is likely a general method for regioselective introduction of a chloride at the 4-position.

Kinetics and Thermodynamics of Halopyridine Scrambling Reactions. By utilizing the much lower solubility of LiF in DMSO in comparison to LiCl, we were able to perform reverse Halex reactions of fluoropyridines to give 4-chloro-substituted products. Given that fluoride and chloride ions were both capable of undergoing S_NAr reactions under these conditions, we hypothesized that *catalytic* halide ion could scramble halogen atoms between halopyridines by a series of reversible S_NAr reactions. Equilibration of chlorofluoropyridines has been previously performed at high temperature (520 °C) with a heterogeneous catalyst by Weigert as a technique to recycle unwanted, overfluorinated Halex products back to the desired mixed chlorofluoropyridines.[32] We were particularly interested in developing a lower temperature method to scramble halopyridines that could be more tolerant of sensitive functional groups. To test this proposal, a homogeneous, equimolar mixture of neat **F$_5$** and **2,4,6-F$_3$** with 2 mol % of *n*-Bu_4PCl (relative to **F$_5$**) was heated at 150 °C for 16 h. ^{19}F NMR spectroscopy showed predominantly unreacted **F$_5$** and **2,4,6-F$_3$**. However, closer inspection showed two small, virtually coupled multiplets at δ −90.7 and −142.7 that indicated the presence of approximately 1 mol % of **2,3,5,6-F$_4$**, at roughly the same level as the amount of *n*-Bu_4PCl catalyst. This suggested that **F$_5$** was able to undergo a regioselective, *stoichiometric* reverse Halex reaction with chloride ion at 150 °C. From Table 2, the calculated $\Delta H^{\ddagger}$ value for S_NAr of chloride ion at the kinetically preferred 4-position of **F$_5$** is 26.1 kcal/mol. The subsequent reverse Halex reaction of **2,3,5,6-F$_4$** at the 2-position had a calculated $\Delta H^{\ddagger}$ value of 33.0 kcal/mol and was not observed at this temperature. The resulting *n*-Bu_4PF[33] from this reverse Halex reaction would instead be expected to react with **2,3,5,6-F$_4$** at the 4-position ($\Delta H^{\ddagger}$ = 12.7 kcal/mol) to regenerate **F$_5$** much more quickly than it would react with **2,4,6-F$_3$** at the 3-position ($\Delta H^{\ddagger}$ = 23.8 kcal/mol). Because of these relative differences in enthalpies of activation, this equilibrium lay toward the starting materials, **F$_5$** and **2,4,6-F$_3$**. In this respect, the reaction of **F$_5$** and **2,4,6-F$_3$** with catalytic chloride ion is a competition experiment which favors starting materials. Consistent with this explanation, the comproportionation of **F$_5$** and **2,4,6-F$_3$** to 2 mol of **2,3,5,6-F$_4$** was endothermic by 1.9 kcal/mol (Table 2) and further suggested that this particular halopyridine scrambling reaction was unfavorable at 150 °C.

To overcome the limited conversion in the reaction of **F$_5$** with **2,4,6-F$_3$**, a more favorable halopyridine scrambling reaction was attempted with a chloropyridine which was more reactive to the fluoride ion liberated by the reverse Halex step. **F$_0$** was chosen as the chloropyridine, due to its high reactivity with fluoride at the 2- and 4-positions. Computations suggested that a reaction would occur between **F$_5$** and **F$_0$**, since $\Delta H^{\ddagger}$ for reaction of fluoride at the 4-position of **F$_0$** (11.5 kcal/mol) was lower than that at the 4-position of **2,3,5,6-F$_4$** (12.7 kcal/mol), and **F$_5$** + **F$_0$** → **2,3,5,6-F$_4$** + **4-F$_1$** was thermodynamically exothermic by 2.7 kcal/mol. When an equimolar mixture of neat **F$_5$** and **F$_0$** was heated with 2 mol % *n*-Bu_4PCl at 160 °C, a mixture of tetrafluoro, trifluoro, difluoro, and monofluoro isomers was observed by gas chromatography and ^{19}F NMR spectroscopy (Table 4). We propose that the

Table 4. Product Distributions (mol %) from Halopyridine Scrambling Reactions of F$_0$ with F$_5$ and 2,4,6-F$_3$, As Determined by ^{19}F NMR

	F$_0$ + F$_5$		**F$_0$ + 2,4,6-F$_3$**	
	1 h	24 h	1 h	24 h
F$_5$	8.8			
2,3,5,6-F$_4$	55.2	53.4		
2,4,6-F$_3$	1.6	1.1	46.3	17.1
2,6-F$_2$	3.3	14.4	31.9	47.6
2,4-F$_2$	8.8	1.1	3.8	6.7
2-F$_1$	12.1	28.9	8.3	20.0
4-F$_1$	9.9	1.1	9.6	8.6

product distribution resulted from a series of halide substitutions involving reverse Halex reactions with high *kinetic* regioselectively at the 4-position along with concomitant forward Halex reactions which approached *thermodynamic* control at extended reaction times (Figure 7). Rapid conversion of **F$_5$** to **2,3,5,6-F$_4$** was observed after only 1 h at 160 °C by reaction of chloride at the kinetically preferred 4-position. No further reaction of **2,3,5,6-F$_4$** occurred even after 48 h at 160 °C. The remaining products were derived from Halex reactions of the liberated fluoride ion, and these regioselectivities were consistent with thermodynamic control at longer reaction times. After 1 h at 160 °C, a 55:45 mixture of **2-F$_1$** and **4-F$_1$** was

DOI: 10.1021/acs.joc.6b01656
J. Org. Chem. XXXX, XXX, XXX−XXX

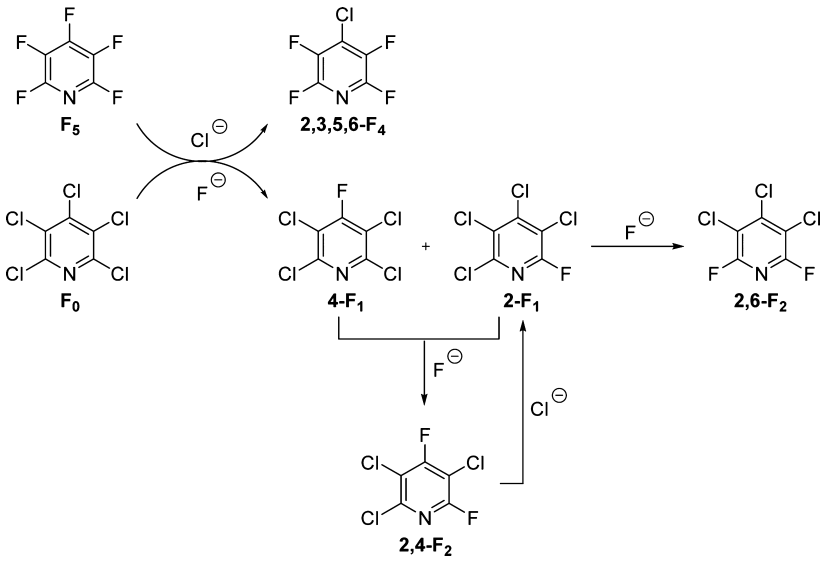

Figure 7. Halopyridine equilibration of $\mathbf{F_5}$ and $\mathbf{F_0}$ using catalytic *n*-Bu_4PCl at 160 °C.

formed, which then equilibrated over 24 h at 160 °C to give a 96:4 mixture of **2-F$_1$** and **4-F$_1$**. As shown in Table 2, the **4-F$_1$** isomer was kinetically favored (by 1.0 kcal/mol), but the **2-F$_1$** regioisomer was thermodynamically favored by 3.4 kcal/mol. On correction for the abundance of ortho C−F positions, a 99:1 ratio of **2-F$_1$** and **4-F$_1$** was calculated at 160 °C on the basis of the computed $\Delta H°$ values, in close agreement with experimental results. Equilibration likely occurred by a Halex reaction of **4-F$_1$** with fluoride to form **2,4-F$_2$**, which can undergo a highly regioselective reverse Halex reaction at the 4-position to generate **2-F$_1$**. The monofluoro products reacted further with fluoride to generate a difluorotrichloropyridine fraction with a 27:73 ratio of **2,6-F$_2$** and **2,4-F$_2$** after 1 h at 160 °C. This ratio increased to 93:7 (**2,6-F$_2$**: **2,4-F$_2$**) over 24 h at 160 °C, presumably via a series of reversible S_NAr reactions. Computationally, **2,6-F$_2$** was significantly more stable than **2,4-F$_2$** by 3.5 kcal/mol (the **2,6-F$_2$**:**2,4-F$_2$** ratio was computed to be 97:3 at 160 °C).

The reaction of $\mathbf{F_0}$ and **2,4,6-F$_3$** with 2 mol % *n*-Bu_4PCl at 160 °C gave analogous results (Table 3). After 1 h, a mixture of **2-F$_1$**, **4-F$_1$**, **2,4-F$_2$**, and **2,6-F$_2$** was observed in addition to starting **2,4,6-F$_3$**. Unreacted $\mathbf{F_0}$ was observable by gas chromatography. Neither tetrafluorochloropyridines nor $\mathbf{F_5}$ was observed, since these products could only result from S_NAr at the much less reactive 3- and 5-positions. The reverse Halex reaction of **2,4,6-F$_3$** with chloride gave the difluoro isomer **2,6-F$_2$**, which is both kinetically and thermodynamically preferred over the **2,4-F$_2$** isomer. The **2,6-F$_2$**:**2,4-F$_2$** ratio remained constant at 88:12 during the 24 h reaction time. The reactivity of **2,4,6-F$_3$** was substantially lower than that of $\mathbf{F_5}$ in halopyridine scrambling reactions with $\mathbf{F_0}$. This reactivity trend was consistent with the calculated 1.1 kcal/mol higher barrier for the reverse Halex reaction of **2,4,6-F$_3$** relative to $\mathbf{F_5}$. Monofluoro products were formed by the reaction of the resulting fluoride ion with $\mathbf{F_0}$ to give a 46:54 mixture of **2-F$_1$** and **4-F$_1$**. This ratio increased to 70:30 **2-F$_1$**:**4-F$_1$** with continued heating for 24 h. The isomerization of **4-F$_1$** to **2-F$_1$** likely occurred by a series of reversible S_NAr reactions with halide ions via **2,4-F$_2$** (Figure 8).

These studies indicated that halide scrambling between chloropyridines and fluoropyridines occurred using 2 mol % *n*-Bu_4PCl at 160 °C to produce mixed chlorofluoropyridines. Substitutions at the 2-, 4-, and 6-positions were observed with a kinetically controlled preference for chloride substituents at the 4-position and a thermodynamic preference for fluorine atoms at the 2- and 6- positions. Under these conditions, no products of substitution at the 3- and 5-positions were observed.

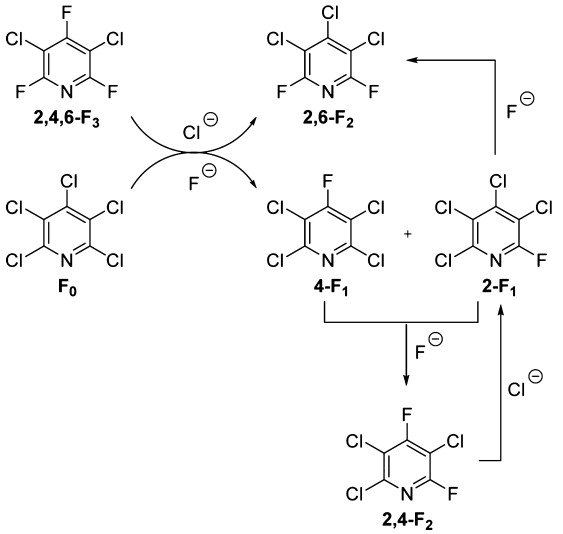

Figure 8. Halopyridine equilibration of **2,4,6-F$_3$** and $\mathbf{F_0}$ using catalytic *n*-Bu_4PCl at 160 °C.

Weigert has previously demonstrated that $\mathbf{F_5}$ and **2,4,6-F$_3$** disproportionate at 520 °C in the presence of Cr_2O_3 to give products which arise from halide exchange at the 3- and 5- as well as 2-, 4-, and 6- positions.[32] A 92% selectivity for products with fluorine atoms at both the 2- and 6-positions was reported. At 520 °C, these product distributions appear to be under thermodynamic control, and all barriers to S_NAr including the 3- and 5-positions are apparently accessible at this temperature. Using the $\Delta H°$ values from our ab initio calculations (Table 2), the mixed chlorofluoropyridine product ratios in the equilibration of a 1:1 mixture of $\mathbf{F_5}$ and **2,4,6-F$_3$** at 520 °C were computed using COPASI (Figure 9).[34] Good agreement between computed and experimental product distributions was obtained. The monochlorotetrafluoropyridine products are

DOI: 10.1021/acs.joc.6b01656
J. Org. Chem. XXXX, XXX, XXX−XXX

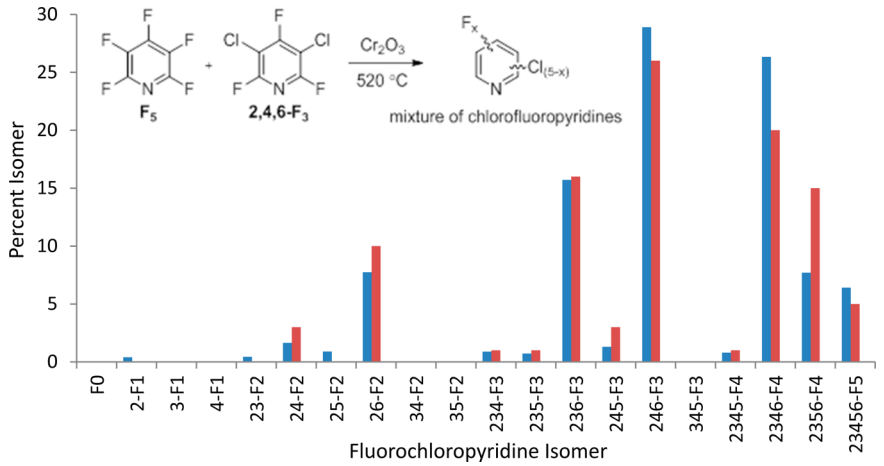

Figure 9. Comparison of the relative thermodynamic product distribution in the equilibration of $\mathbf{F_5}$ and **2,4,6-$\mathbf{F_3}$** for experimental (red)[33] and computed (blue) data at 520 °C.

formed as a 1.3:1 mixture of **2,3,5,6-$\mathbf{F_4}$** and **2,3,4,6-$\mathbf{F_4}$**, consistent with their calculated $\Delta\Delta H°$ value of 0.9 kcal/mol. This regioselectivity is in contrast with our observed regiospecific formation of **2,3,5,6-$\mathbf{F_4}$** under kinetically controlled conditions at 160 °C. Similarly, **2,4,6-$\mathbf{F_3}$** was isomerized to a 1.6:1 mixture of **2,4,6-$\mathbf{F_3}$** and **2,3,6-$\mathbf{F_3}$**, consistent with the calculated $\Delta\Delta H°$ of 2.1 kcal/mol between these two isomers.

Factors Controlling Thermodynamics. Our experimental results showed a strong thermodynamic preference for pentahalopyridine isomers which contain fluorine atoms at the 2- and 6-positions. We postulated that the relative strength of the C−Cl and C−F bonds at the 2- and 6-positions could be the driving force for this selectivity. Houk has reported that the weakest C−halogen bonds preferentially react in Suzuki coupling reactions of polyhalogenated heterocycles, on the basis of calculated homolytic bond dissociation energies (BDEs).[35] In particular, C−Cl bonds at the 2-position were calculated to be more than 3 kcal/mol weaker than C−Cl bonds at the other positions. Similarly, C−Br bonds at the 2-position were also calculated to have the lowest BDEs in comparison to C−Br bonds at the 3- and 4-positions.[35] We calculated that BDEs for C−F bonds at the 2-position, unlike the corresponding C−Cl and C−Br bonds, were essentially the same as the computed BDEs of C−F bonds at the 3- and 4-positions. For example, the C−Cl bond in 2-chloropyridine was calculated to be 3.9 and 2.9 kcal/mol weaker than the C−Cl bonds in 3-chloropyridine and 4-chloropyridine, respectively (Table 5, entries 1−3). In contrast, the calculated C−F BDEs of the three fluoropyridine isomers were all within 0.7 kcal/mol.

We calculated all of the homolytic C−X bond dissociation enthalpies at the G3MP2B3* level for the 20 possible mixed chlorofluoropyridines in the Halex reaction of $\mathbf{F_0}$ (Supporting Information). Trends observed with pentahalopyridines were similar to those seen with monohalopyridines. Specifically for $\mathbf{F_0}$, the C−Cl bond at the 2-position was 3−4 kcal/mol weaker than the C−Cl bonds at the 3- and 4-positions (Table 5, entry 4). By comparison, the C2−F bond in $\mathbf{F_5}$ was calculated to be the strongest C−F bond and was 2.0 and 0.5 kcal/mol stronger than the C−F bonds at the 3- and 4-positions of $\mathbf{F_5}$, respectively. For all 20 pentahalopyridines, calculated BDEs for C−Cl bonds averaged 96.4, 99.5, and 100.1 kcal/mol at C2, C3, and C4, respectively. At each ring position, the C−Cl BDEs had a small standard deviation of 0.4 kcal/mol, which suggested that the position of the chloride on the pyridine ring was the primary determinant of the strength of these C−Cl bonds. Calculated average BDEs for C−F bonds in these 20 pentahalopyridines spanned a much narrower range (127.2, 125.2, and 126.7 kcal/mol at C2, C3, and C4, respectively), but standard deviations at each position were significantly larger for C−F bonds than for their corresponding C−Cl bonds. This suggested that neighboring halogen substituents, not ring position, might be the dominant factor in determining the strength of the C−F bonds in this system.

To test this hypothesis, we performed a series of calculations on simple halobenzene structures to eliminate the effect of pyridine nitrogen and investigate solely the effect of ortho halogen substituents on C−-X BDEs (Table 5, entries 5−10). In this respect, ortho does not refer to the 2-position but refers to atoms ortho to the particular C−X bond in question. For chlorobenzenes, BDEs of C−Cl bonds spanned a narrow 99.9−100.5 kcal/mol range and showed no effect on the presence of ortho H, F, or Cl substituents. However, calculated BDEs in these halobenzenes showed a weakening of the C−F bond with increasing numbers of ortho fluoride substituents. The presence of ortho Cl substituents had no effect on the calculated C−F BDE (entries 5, 6, and 8). However, the C−F BDEs decreased with an increasing number of fluoride substituents ortho to the C−F bond. For example, the C−F BDE in fluorobenzene was calculated to be 128.4 kcal/mol (entry 5). The presence of one ortho fluorine (entries 7 and 9) decreased the C−F BDE to 126.8 kcal/mol. The two fluorine atoms ortho to a C−F bond as in 1,2,3-trifluorobenzene (entry 10) further decreased the C−F BDE at the 2-position to 125.5 kcal/mol. Each ortho fluorine substituent weakened the C−F bond by ∼1.5 kcal/mol. These trends were comparable to the relative effects of the nature of the ortho halogen substituent on the relative strengths of C−F and C−Cl bonds in pentahalopyridines. In all cases studied, fluorine atoms ortho to a C−F bond led to a decrease in its BDE. In the stepwise Halex reactions of $\mathbf{F_0}$ to ultimately give $\mathbf{F_5}$, the average $\Delta H°$ values for each sequential fluorination step were 17.1, 16.3, 16.2, 15.5, and 15.0 kcal/mol for the first, second, third, fourth, and fifth substitutions, respectively. These reactions become less exothermic with increasing degree of fluorine incorporation due to this ortho fluorine effect.

With knowledge of the ortho fluorine effect on C−F bonds, the 2-position effect on C−Cl bonds, and the fact that every sequential fluorine addition is significantly exothermic, we attempted to describe the relative G3MP2B3* $\Delta H°$ values of

DOI: 10.1021/acs.joc.6b01656
J. Org. Chem. XXXX, XXX, XXX−XXX

Table 5. G3MP2B3* Calculated C−F and C−Cl Homolytic Bond Dissociation Enthalpies (in kcal/mol) for Monohalopyridine Isomers, F_0 and F_5, and a Series of Halobenzenes

entry	compound	X = Cl C-Cl BDE	X = F C-F BDE	Δ_{BDE} [a]
1		95.8	128.3	32.5
2		99.7	127.6	27.9
3	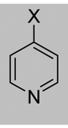	98.7	127.9	29.2
4	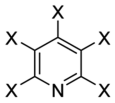	96.4 (C2) 99.5 (C3) 100.1 (C4) **F_0**	127.2 (C2) 125.2 (C3) 126.7 (C4) **F_5**	30.8 (C2) 25.7 (C3) 26.6 (C4)
5		99.9	128.4	28.5
6		99.9	128.1	28.2
7		99.9	126.8	26.9
8		100.2	128.0	27.8
9	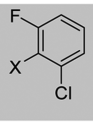	100.4	126.8	26.4
10	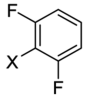	100.5	125.5	25.0

[a] Δ_{BDE} = (C−F BDE) − (C−Cl BDE).

all 20 mixed chlorofluoropyridine structures using three simple factors: (1) the number of fluorine atoms in the molecule ($\sum$F), (2) the number of fluorine atoms at the C2/C6 positions ($\sum F_{C2/C6}$), and (3) the number of pairs of fluorine atoms which are ortho to one another ($\sum$ortho F−F pairs) (see Figure 10 and the Supporting Information). As discussed above, C2−Cl bonds are 3−4 kcal/mol weaker than C−Cl bonds at the other positions. In addition, the presence of a fluorine atom in an ortho relationship to a C−F bond leads to a weakening of that C−F bond by approximately 1.5 kcal/mol. The G3MP2B3* $\Delta H°$ values from Table 2 were fit using these three variables (Figure 11, eq 1), and a nearly perfect agreement was observed.

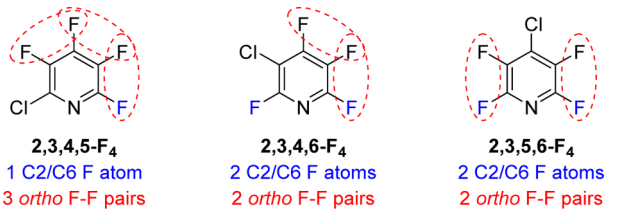

Figure 10. Illustration of number of C2/C6 fluorine atoms and number of ortho F−F pairs for the three possible chlorotetrafluoropyridine isomers.

$$\Delta H° = \{-15.29 \sum \mathrm{F}\} - \{4.16 \sum \mathrm{F}_{C2/C6}\} + \{1.32 \sum \text{ortho F−F pairs}\} \quad (1)$$

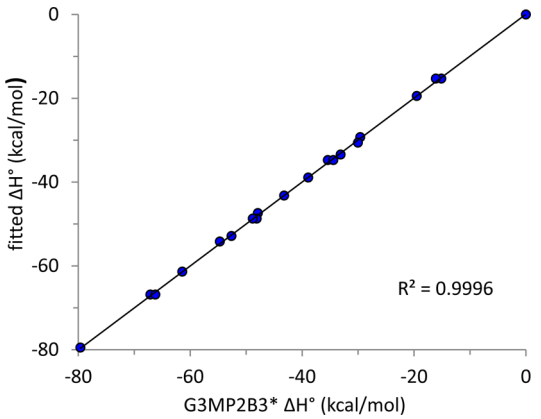

Figure 11. Comparison of fitted $\Delta H°$ values using eq 1 with calculated $\Delta H°$ using the G3MP2B3* method for all 20 possible chlorofluoropyridines in the Halex reaction of F_0 to F_5.

Equation 1 shows the critical importance of the 2-position and the smaller but significant contribution of ortho F−F pairs on $\Delta H°$ values. As the reaction progresses from F_0 to F_5, greater fluorination leads to the presence of more ortho F−F pairs, thus weakening the remaining C−F bonds that eventually form. One effect of this thermodynamic situation is that equilibration of mixtures of chlorofluoropyridines will be biased toward formation of less fluorinated species due to fewer ortho F−F pairs, in agreement with our experimental results (Table 4).

CONCLUSIONS

The Halex reaction of pentachloropyridine with fluoride ion was studied experimentally and computationally. The ab initio G3MP2B3 method was modified because geometry optimizations with the small 6-31G* basis set failed due to the lack of diffuse functions, often a requirement of anionic transition states. Experimental regioselectivities were consistent with kinetic control with the 4-position moderately preferred over the 2-position; the calculated S_NAr transition states supported this trend. It was thought that the reverse Halex reaction of fluoropyridines with chloride sources was possible, and it was indeed demonstrated by using precipitation of LiF in DMSO as a driving force. Calculations suggested that the reverse Halex reaction would be highly regioselective, and experiments showed only substitution by chloride at the 4-position, consistent with kinetic control. Scrambling of halide ions between chlorofluoropyridines was found to occur using

DOI: 10.1021/acs.joc.6b01656
J. Org. Chem. XXXX, XXX, XXX−XXX

catalytic quantities of *n*-Bu_4PCl, and the products of these reactions were shown to result from a combination of kinetic and thermodynamic control. The relative enthalpic reaction thermodynamics of all possible chlorofluoropyridine structures could be predicted as a function of three variables: the number of fluorine atoms in the molecule, the number of fluorine atoms at the C2/C6 positions, and the number of pairs of fluorine atoms which are ortho to one another.

COMPUTATIONAL DETAILS

Expanded details of methods and comparisons are provided in the Supporting Information. Computations used the Gaussian03 program.[36] The G3 suite of programs[37] has been developed for extremely high level and accurate predictions of energies and is considered a "kcal/mol accurate" method. G3 procedures are one set among others[38] that utilize extrapolation procedures for accurate energy calculations. We proceeded to utilize both the standard DFT method B3LYP[39] with the large basis set 6-311+G**,[40] which we denote as B3LYP/6-311+G**, and the G3MP2B3* level of theory. Initially, the structures were optimized at the B3LYP/6-311+G** level of theory where energies and thermal/entropic corrections could be determined. Since Halex reactions are typically performed in polar solvents such as DMSO, the polarized continuum model (PCM)[41] was included in these calculations (B3LYP, G3MP2B3), with the solvent DMSO (dielectric constant ε = 46.7). Due to many complications associated with entropy, we have focused on the enthalpy of activation and enthalpy of reaction for the Halex reaction solvated in DMSO utilizing the "naked fluoride" anion.[42,43]

The individual components of the modified G3MP2B3 method were computed on the basis of the B3LYP/6-311+G** optimized geometries. The G3MP2B3* energies are defined as

$$E\{\mathrm{G3MP2B3^*}\} = E\{\mathrm{QCISD(T)/6\text{-}31{+}G^*}\} + \Delta E\{\mathrm{MP2^*}\}$$

where

$$\Delta E\{\mathrm{MP2^*}\} = E\{\mathrm{MP2/6\text{-}311{+}{+}g(2df,2p)}\} - E\{\mathrm{MP2/6\text{-}31{+}G^*}\}$$

Our enthalpies calculated using the G3MP2B3* method were corrected for the enthalpy (298 K) from the B3LYP calculation:

$$H\{\mathrm{G3MP2B3^*}\} = E\{\mathrm{G3MP2B3^*}\} + H\{\mathrm{B3LYP/6\text{-}311{+}G^{**}}\} - E\{\mathrm{B3LYP/6\text{-}311{+}G^{**}}\}$$

It should be noted that the B3LYP/6-311+G** method provides results which are consistent with the high-level G3MP2B3* method.

ASSOCIATED CONTENT

Supporting Information

The Supporting Information is available free of charge on the ACS Publications website at DOI: 10.1021/acs.joc.6b01656.

Details on eq 1 and Figure 11, a complete set of energies and Cartesian coordinates for the computational data, further details on the fitting of the equilibrium constant data (Figure 9), and experimental procedures for Halex and reverse Halex reactions along with ^{19}F NMR spectra (PDF)

AUTHOR INFORMATION

Corresponding Authors

*E-mail for R.D.J.F.: froeserd@dow.com.
*E-mail for G.T.W.: whitekgt2@dow.com.

Notes

The authors declare no competing financial interest.

REFERENCES

(1) Müller, K.; Faeh, C.; Diedrich, F. *Science* **2007**, *317*, 1881.
(2) Jeschke, P. *Pest Manage. Sci.* **2010**, *66*, 10.
(3) Hiyama, T. Biologically active organofluorine compounds. In *Organofluorine Compounds: Chemistry and Applications*; Springer: Berlin, 2000; pp 137−182.
(4) Hagmann, W. K. *J. Med. Chem.* **2008**, *51*, 4359.
(5) Fujiwara, T.; O'Hagan, D. *J. Fluorine Chem.* **2014**, *167*, 16.
(6) Kirk, K. L. *Org. Process Res. Dev.* **2008**, *12*, 305.
(7) Adams, D. J.; Clark, J. H. *Chem. Soc. Rev.* **1999**, *28*, 225.
(8) Finger, G. C.; Kruse, C. W. *J. Am. Chem. Soc.* **1956**, *78*, 6034.
(9) (a) Sun, H.; DiMagno, S. G. *Angew. Chem., Int. Ed.* **2006**, *45*, 2720. (b) Allen, L. J.; Muhuhi, J. M.; Bland, D. C.; Merzel, R.; Sanford, M. S. *J. Org. Chem.* **2014**, *79*, 5827. (c) Allen, L. J.; Lee, S. H.; Cheng, Y.; Hanley, P. S.; Muhuhi, J. M.; Kane, E.; Powers, S. L.; Anderson, J. E.; Bell, B. M.; Roth, G. A.; Sanford, M. S.; Bland, D. C. *Org. Process Res. Dev.* **2014**, *18*, 1045. (d) Schimler, S. D.; Ryan, S. J.; Bland, D. C.; Anderson, J. E.; Sanford, M. S. *J. Org. Chem.* **2015**, *80*, 12137.
(10) Bunnett, J. F.; Zahler, R. E. *Chem. Rev.* **1951**, *49*, 273.
(11) Paradisi, C. In *Comprehensive Organic Synthesis*; Trost, B. M., Ed.; Pergamon Press: Oxford, U.K., 1991; Vol. *4*, Chapter 2.1.
(12) Shiley, R. H.; Dickerson, D. R.; Finger, G. C. *J. Fluorine Chem.* **1972**, *2*, 19.
(13) Trademark of The Dow Chemical Company ("Dow") or an affiliated company of Dow.
(14) Epp, J. B.; Gast, R. E.; Schmitzer, P. R.; Irvine, N. M.; Lo, W. C.; Richburg, J. S.; Lowe, C. T.; Ruiz, J. M.; Alexander, A. L.; Siddall, T. L.; Brewster, W. K.; Webster, J. D.; Bryan, K.; Weimer, M. R.; Buysse, A. M.; Yerkes, C. N.; Satchivi, N.; Daeuble, J. F.; Balko, T. W.; Whiteker, G. T.; Fields, S. C.; Green, R. A.; Renga, J. *Bioorg. Med. Chem.* **2016**, *24*, 362.
(15) (a) Sasson, Y.; Zoran, A. WO 2000044724, 2000. (b) Wilson, C. A.; Fung, A. P. U.S. Patent 4,746,744, 1988. (c) Banks, R. E.; Haszeldine, R. N.; Latham, J. V.; Young, I. M. *J. Chem. Soc.* **1965**, 594. (d) Chambers, R. D.; Hutchinson, J.; Musgrave, W. K. R. *J. Chem. Soc.* **1964**, 3573.
(16) The shorthand nomenclature indicates the positions of the fluorine atoms. Positions that are not denoted imply a chloride substituent at those positions. For example, **2,4,6-F_3** refers to 3,5-dichloro-2,4,6-trifluoropyridine.
(17) Orvik, J. A.; Fung, A. P.; Love, J.; Dietsche, T. J. U.S. Patent 4,766,219, 1988.
(18) Aksenov, V. V.; Vlasov, V. M.; Moryakina, I. M.; Rodionov, P. P.; Fadeeva, V. P.; Chertok, V. S.; Yakobson, G. G. *J. Fluorine Chem.* **1985**, *28*, 73.
(19) Middleton, W. J. *Org. Synth.* **1986**, *64*, 221.
(20) Unreacted pentachloropyridine is not detectable by this analysis.
(21) Flowers, W. T.; Haszeldine, R. N.; Majid, S. A. *Tetrahedron Lett.* **1967**, *8*, 2503.
(22) (a) Liljenberg, M.; Brinck, T.; Herschend, B.; Rein, T.; Rockwell, G.; Svensson, M. *J. Org. Chem.* **2010**, *75*, 4696. (b) Liljenberg, M.; Brinck, T.; Herschend, B.; Rein, T.; Rockwell, G.; Svensson, M. *Tetrahedron Lett.* **2011**, *52*, 3150. (c) Fernández, I.; Frenking, G.; Uggerud, E. *J. Org. Chem.* **2010**, *75*, 2971.
(23) Pliego, J. R., Jr.; Piló-Veloso, D. *Phys. Chem. Chem. Phys.* **2008**, *10*, 1118.
(24) Muir, M.; Baker, J. *J. Fluorine Chem.* **2005**, *126*, 727.
(25) Glukhovtsev, M. N.; Bach, R. D.; Laiter, S. *J. Org. Chem.* **1997**, *62*, 4036.
(26) For optimization and convergence problems of G3MP2B3, see: Islam, S. M.; Poirier, R. A. *J. Phys. Chem. A* **2007**, *111*, 13218.
(27) The transition states are all anionic, and it is well-known that diffuse functions would help in these types of calculations. The recently developed G4 methods optimize the geometries with a larger basis set {B3LYP/6-31G(2df,p)}, although this method still lacks diffuse functions: Curtiss, L. A.; Redfern, P. C.; Raghavachari, K. *J. Chem. Phys.* **2007**, *126*, 084108. A simple set of test calculations demonstrated that, with the B3LYP method, 6-31G(d) and 6-31G(2df,p) failed while 6-31+G(d) and 6-311+G(d,p) were successful in optimizing these types of transition states.
(28) Manuscript in preparation.

DOI: 10.1021/acs.joc.6b01656
J. Org. Chem. XXXX, XXX, XXX−XXX

(29) (a) *IUPAC Solubility Data Series*; Cohen-Adad, R., Lorimer, J. W., Eds.; Pergamon Press: Oxford, U.K., 1991; Vol. *47*. (b) Stubblefield, C. B.; Bach, R. O. *J. Chem. Eng. Data* **1972**, *17*, 491. (c) Krumgalz, B. S. *Mineral Solubility in Water at Various Temperatures*; Israel Oceanographic and Limnological Research Ltd.: Haifa, Israel, 1994.
(30) (a) Bolli, C.; Gellhaar, J.; Jenne, C.; Keßler, M.; Scherer, H.; Seeger, H.; Uzun, R. *Dalton Trans.* **2014**, *43*, 4326. (b) Martinsen, A.; Songstad, J. *Acta Chem. Scand.* **1977**, *31a*, 645. (c) Berkessel, A.; Brandenburg, M. *Org. Lett.* **2006**, *8*, 4401.
(31) Vaganova, T. A.; Kusov, S. Z.; Rodionov, V. I.; Shundrina, I. K.; Malykhin, E. V. *Russ. Chem. Bull.* **2007**, *56*, 2239.
(32) Weigert, F. J. *J. Fluorine Chem.* **1991**, *53*, 33.
(33) Seto, H.; Qian, Z.; Yoshioka, H.; Uchibori, Y.; Umeno, M. *Chem. Lett.* **1991**, *20*, 1185.
(34) COPASI 4.11: Hoops, S.; Sahle, S.; Gauges, R.; Lee, C.; Pahle, J.; Simus, N.; Singhal, M.; Xu, L.; Mendes, P.; Kummer, U. *Bioinformatics* **2006**, *22*, 3067.
(35) Garcia, Y.; Schoenebeck, F.; Legault, C. Y.; Merlic, C. A.; Houk, K. N. *J. Am. Chem. Soc.* **2009**, *131*, 6632.
(36) Frisch, M. J.; Trucks, G. W.; Schlegel, H. B.; Scuseria, G. E.; Robb, M. A.; Cheeseman, J. R.; Montgomery, J. A., Jr.; Vreven, T.; Kudin, K. N.; Burant, J. C.; Millam, J. M.; Iyengar, S. S.; Tomasi, J.; Barone, V.; Mennucci, B.; Cossi, M.; Scalmani, G.; Rega, N.; Petersson, G. A.; Nakatsuji, H.; Hada, M.; Ehara, M.; Toyota, K.; Fukuda, R.; Hasegawa, J.; Ishida, M.; Nakajima, T.; Honda, Y.; Kitao, O.; Nakai, H.; Klene, M.; Li, X.; Knox, J. E.; Hratchian, H. P.; Cross, J. B.; Bakken, V.; Adamo, C.; Jaramillo, J.; Gomperts, R.; Stratmann, R. E.; Yazyev, O.; Austin, A. J.; Cammi, R.; Pomelli, C.; Ochterski, J. W.; Ayala, P. Y.; Morokuma, K.; Voth, G. A.; Salvador, P.; Dannenberg, J. J.; Zakrzewski, V. G.; Dapprich, S.; Daniels, A. D.; Strain, M. C.; Farkas, O.; Malick, D. K.; Rabuck, A. D.; Raghavachari, K.; Foresman, J. B.; Ortiz, J. V.; Cui, Q.; Baboul, A. G.; Clifford, S.; Cioslowski, J.; Stefanov, B. B.; Liu, G.; Liashenko, A.; Piskorz, P.; Komaromi, I.; Martin, R. L.; Fox, D. J.; Keith, T.; Al-Laham, M. A.; Peng, C. Y.; Nanayakkara, A.; Challacombe, M.; Gill, P. M. W.; Johnson, B.; Chen, W.; Wong, M. W.; Gonzalez, C.; Pople, J. A. *Gaussian 03, Revision C.02*; Gaussian, Inc., Wallingford, CT, 2004.
(37) Curtiss, L. A.; Redfern, P. C.; Raghavachari, K.; Rassolov, V.; Pople, J. A. *J. Chem. Phys.* **1999**, *110*, 4703.
(38) Froese, R. D. J.; Humbel, S.; Svensson, M.; Morokuma, K. *J. Phys. Chem. A* **1997**, *101*, 227.
(39) (a) Becke, A. D. *J. Chem. Phys.* **1993**, *98*, 5648. (b) Lee, C.; Yang, W.; Parr, R. G. *Phys. Rev. B: Condens. Matter Mater. Phys.* **1988**, *37*, 785. (c) Miehlich, B.; Savin, A.; Stoll, H.; Preuss, H. *Chem. Phys. Lett.* **1989**, *157*, 200.
(40) (a) Ditchfield, R.; Hehre, W. J.; Pople, J. A. *J. Chem. Phys.* **1971**, *54*, 724. (b) Hehre, W. J.; Ditchfield, R.; Pople, J. A. *J. Chem. Phys.* **1972**, *56*, 2257. (c) Gordon, M. S. *Chem. Phys. Lett.* **1980**, *76*, 163. (d) McLean, A. D.; Chandler, G. S. *J. Chem. Phys.* **1980**, *72*, 5639. (e) Krishnan, R.; Binkley, J. S.; Seeger, R.; Pople, J. A. *J. Chem. Phys.* **1980**, *72*, 650.
(41) (a) Miertus, S.; Scrocco, E.; Tomasi, J. *Chem. Phys.* **1981**, *55*, 117. (b) Tomasi, J.; Mennucci, B.; Cancès, E. *J. Mol. Struct.: THEOCHEM* **1999**, *464*, 211 and references therein. (c) Pliego, J. R., Jr.; Riveros, J. M. *Chem. Phys. Lett.* **2002**, *355*, 543.
(42) Smyth, T. P.; Carey, A.; Hodnett, B. K. *Tetrahedron* **1995**, *51*, 6363.
(43) Solvation could play a key role, and one would anticipate that the solvation model could affect the absolute barrier of the reaction, but it should not affect selectivities or the relative ordering of reaction barriers. Determining an absolute barrier is complicated, as the enthalpy has both ion pairing and ion−solvent interactions while the entropy of activation is convoluted due to solvent reorganization around the ion. This complexity explains why a range of experimental reaction rates is observed when fluoride is used as a nucleophile.

DOI: 10.1021/acs.joc.6b01656
J. Org. Chem. XXXX, XXX, XXX−XXX